

# Photoinduced Alignment of Ferroelectric Liquid Crystals Using Azobenzene Polymer Networks of Chiral Polyacrylates and Polymethacrylates

Steve Leclair,<sup>†</sup> Lizamma Mathew,<sup>†</sup> Martin Giguère,<sup>‡</sup> Shahrokh Motallebi,<sup>‡</sup> and Yue Zhao<sup>\*,†</sup>

Département de Chimie, Université de Sherbrooke, Sherbrooke, Québec, Canada J1K 2R1, and St-Jean PhotoChemicals, 725 Trotter, St-Jean-sur-Richelieu, Québec, Canada J3B 8J8

Received June 27, 2003; Revised Manuscript Received September 19, 2003

**ABSTRACT:** Two chiral dimethacrylate and one chiral diacrylate monomer containing an azobenzene group were synthesized and dissolved in a commercial ferroelectric liquid crystal (FLC) host. With two of the monomers, thermally induced radical polymerization with the mixture exposed to linearly polarized irradiation results in a bulk alignment of FLC in the direction perpendicular to the polarization of irradiation light as a result of the photoinduced orientation of azobenzene groups related to the trans–cis isomerization. The monomer that is most effective for photoalignment of FLC displays a polymer network formed by strings of colloidal particles (~250 nm in diameter), which exerts a commanding effect on the alignment of FLC as being able to reorient the FLC by changing the polarization direction of subsequent irradiation. The study suggests that the network of colloidal particles is isotropic and that the photoalignment of azobenzene moieties on the large surface of the network dictates the alignment of FLC.

## Introduction

Polymer-stabilized liquid crystals (PSLC) refer to low-molar-mass liquid crystals (LC) whose bulk alignment or texture is stabilized by a low-concentration polymer network.<sup>1–4</sup> PSLC based on nematic,<sup>2</sup> cholesteric,<sup>1</sup> and ferroelectric liquid crystals (FLC)<sup>2,3</sup> have been studied. In all cases, the LC alignment or texture was first obtained by surface orientation layers or an electric field, followed by polymerization of a monomer dissolved in the LC host. The polymer network formed in the aligned LC host can be anisotropic and, in turn, stabilize the LC alignment or texture. Potential applications of PSLC for displays and electrically switchable optical devices have been demonstrated.<sup>1,2</sup> In the case of polymer-stabilized FLC, another interest is to improve the shock resistance of surface-stabilized FLC cells.<sup>4</sup>

In recent years, azobenzene-containing polymers, including amorphous,<sup>5,6</sup> liquid crystalline,<sup>7–10</sup> and elastomers,<sup>11–13</sup> have attracted a great deal of attention due to their potential utility in holographic storage as well as other optical and photonic applications. Being motivated by this, our group has been exploiting a new type of PSLC, in which the polymer network bears the azobenzene chromophore.<sup>14–18</sup> We showed that the presence of an azobenzene polymer in PSLC made possible the use of the reversible trans–cis photoisomerization as well as the related photoalignment of azobenzene to affect or induce the LC orientation.<sup>14–18</sup> Indeed, when a diacrylate monomer containing an azobenzene moiety is polymerized under linearly polarized irradiation, either in the nematic<sup>15</sup> or isotropic phase,<sup>16</sup> the azobenzene network formed can be anisotropic and induce a stable bulk alignment of the LC in the nematic phase in the absence of rubbed surfaces.

More recently, we reported that azobenzene polymer networks could also be used to optically align FLC.<sup>17,18</sup> In the latter case, however, an increased segregation of the polymer network from the FLC host was observed in aligned samples in the ferroelectric chiral smectic-C ( $S^*_C$ ) phase,<sup>18</sup> giving rise to the formation of thick polymer threads parallel to the FLC alignment direction. Although the bulk alignment of FLC remains, such a large-scale phase separation is not desirable because of the resulting inhomogeneity. In view of the fundamental interest and technological importance of FLC, we have undertaken a systematic investigation to fully assess this optical and rubbing-free approach. As a matter of fact, much effort has been devoted to the development of new alignment methods, other than surface-stabilized FLC.<sup>19</sup> These include polymer-dispersed FLC<sup>20</sup> microphase-stabilized FLC<sup>21</sup> and ferroelectric elastomers,<sup>22,23</sup> for which a mechanical shear is generally employed to induce the alignment.

All azobenzene monomers used in our previous studies are achiral diacrylates. In this paper, we report on the synthesis of a number of chiral azobenzene diacrylate and dimethacrylate monomers as well as the investigation on their use to induce optically aligned FLC without the use of surface orientation layers. It was expected that the chirality in the azobenzene polymer network may improve the compatibility with the FLC in the chiral  $S^*_C$  phase. By doing so, there may be stronger interactions between the azobenzene groups and the surrounding FLC molecules, which facilitate the bulk alignment of FLC through the action of the photoactive azobenzene moieties.

## Experimental Section

**1. Materials.** Aminobenzoic acid (99%), sulfamic acid (98%), sodium acetate trihydrate (99%), ammonium hydroxide (28–30%), phenyldiethanolamine (97%), (s)-(+)-1-bromo-2-methylbutane (99%), 1,8-diazabicyclo[5.4.0]undec-7-ene (98%), methacrylic anhydride (94%), 2,6-di-*tert*-butyl-4-methylphenol (98%),

<sup>†</sup> Université de Sherbrooke.

<sup>‡</sup> St-Jean PhotoChemicals.

\* Corresponding author: e-mail yue.zhao@usherbrooke.ca.

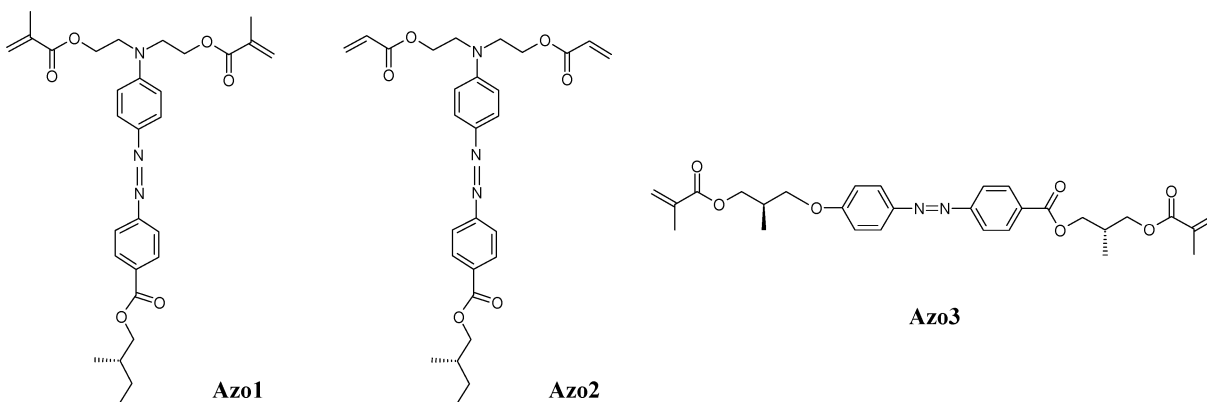
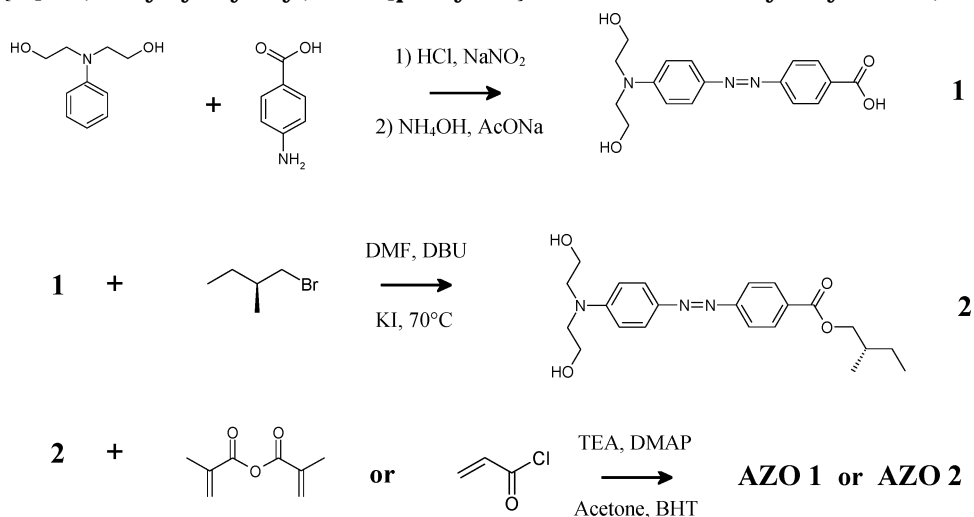


**Figure 1.** Chemical structures of chiral azobenzene monomers.

**Scheme 1. Synthetic Route to Azobenzene Monomers of 4-(4-[Bis-(2-(2-methylacryloyloxy)ethyl)amino]phenylazo)benzoic Acid 2-Methylbutyl Ester (Azo1) and 4-[4-[Bis(2-acryloyloxyethyl)amino]phenylazo]benzoic Acid 2-Methylbutyl Ester (Azo2)**



triethylamine (99%), 4-(dimethylamino)pyridine (99%), acryloyl chloride (96%), and (*s*)-(+)-3-bromo-2-methyl-1-propanol (97%) were used as received from Aldrich. Hydrochloric acid (EMD, 36–38%), sodium nitrite (BDH, 97%), potassium iodide (BDH, 99%), sodium hydroxide (Fisher, 98%), acetic acid (Fisher, 99%), phenol (Lancaster, 99%), and anhydrous potassium carbonate (BDH, 99%) were also used as received. 2,2'-Azobis(isobutyronitrile) (AIBN, Polysciences) was recrystallized from ethanol prior to use. All solvents were commercially available and used as received, except THF which was dried by distillation from sodium and benzophenone under  $N_2$ .

The ferroelectric liquid crystal (FLC) mixture used was Felix-SCE8 purchased from Clariant. It has the following phase transitions:  $C_r -40\text{ }^\circ\text{C}$   $S_C^* 60\text{ }^\circ\text{C}$   $S_A 80\text{ }^\circ\text{C}$   $N^* 102\text{ }^\circ\text{C}$  I. The spontaneous polarization and rotational viscosity of the FLC measured at  $25\text{ }^\circ\text{C}$  are  $-4.5\text{ nC/cm}^2$  and  $76\text{ mPa}$ , respectively (data provided by Clariant).

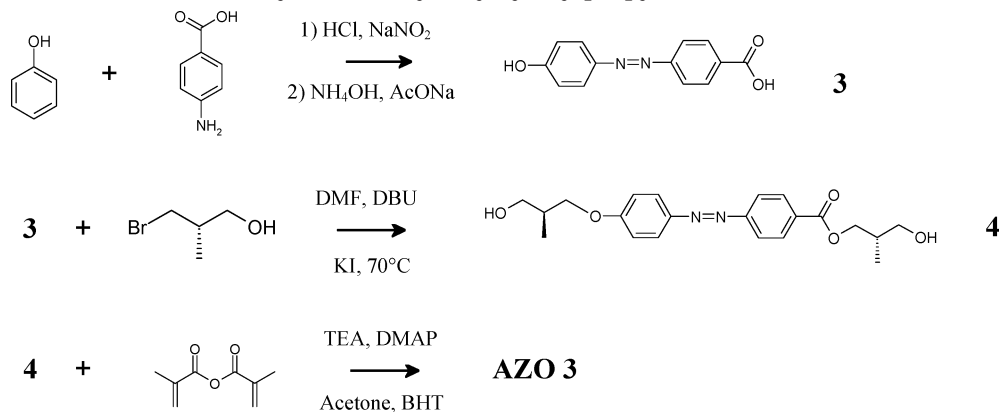
**2. Synthesis of Chiral Azobenzene Monomers.** The chemical structures of the monomers synthesized are shown in Figure 1, including two dimethacrylates (Azo1 and Azo3) and one diacrylates (Azo2). Azo1 and Azo2 have one chiral center and the azobenzene moiety in the side group, while Azo3 has two chiral centers per molecule and the azobenzene moiety in the main chain. Their synthetic routes are depicted in Schemes 1 and 2, with more details given below.

**2.1. Preparation of Azo1 and Azo2. Synthesis of 4-[4-[Bis(2-hydroxyethyl)amino]phenylazo]benzoic Acid (1):** Aminobenzoic acid (24.5 g, 175 mmol) was dissolved in a mixture of water (344 g) and HCl (60.4 g, 613 mmol) and cooled in an ice-acetone bath under stirring. A cold solution of  $NaNO_2$  (13.15 g, 185 mmol) in water (25 g) was added drop by drop to keep the temperature under  $5\text{ }^\circ\text{C}$ , and sulfamic acid

(1.0 g, 0.10 mmol) was then added to neutralize the oxidant. Then the solution was added drop by drop to a cold mixture of AcONa (24.1 g, 175 mmol),  $NH_4OH$  (42.3 g, 350 mmol), and phenyldiethanolamine (32.7 g, 175 mmol) dissolved in water (335 g). The reaction lasted 1 h at room temperature. Afterward, the product was filtered and rinsed with water and dried. An orange powder was obtained with a yield of 56%; mp: decomposed before melting. MS (*m/e*): 329 ( $M^+$ ).  $\lambda_{max}$  (in THF): 444 nm.  $^1H$  NMR: 3.51–3.61 (m,  $N(CH_2CH_2OH)_2$ , 8H), 6.86 (d,  $J = 9.3\text{ Hz}$ , 2 aromatic H ortho to  $N(CH_2)_2$ ), 7.77 (d,  $J = 8.7\text{ Hz}$ , 4 aromatic H ortho to  $N=N$ ), 8.03 (d,  $J = 8.5\text{ Hz}$ , 2 aromatic H ortho to  $C(O)OH$ ).

**Synthesis of 4-[4-[Bis(2-hydroxyethyl)amino]phenylazo]benzoic Acid 2-Methylbutyl Ester (2):** 4-[4-[Bis(2-hydroxyethyl)amino]phenylazo]benzoic acid (1.65 g, 5 mmol), (*s*)-(+)-1-bromo-2-methylbutane (1.51 g, 10 mmol), and potassium iodide (1.24 g, 7.5 mmol) were first dissolved in DMF (120 mL). Then, 1,8-diazabicyclo[5.4.0]undec-7-ene (2.66 g, 17.5 mmol) was added under stirring. The solution was stirred and heated to  $70\text{ }^\circ\text{C}$  for 48 h. The cooled solution was extracted with dichloromethane and washed with water and sodium hydroxide (1 N). The product was purified by column chromatography on silica gel (eluent: acetone/hexane = 4.5/5.5), giving an orange solid with a yield of 50%; mp:  $100.2\text{ }^\circ\text{C}$ . MS (*m/e*): 399 ( $M^+$ ).  $\lambda_{max}$  (in THF): 442 nm.  $^1H$  NMR: 0.96–1.04 (m,  $CH_3CH_2CH(CH_3)CH_2$ , 6H), 1.26–1.54 (m,  $CH_3CH_2CH(CH_3)CH_2$ , 2H), 1.86 (m,  $CH_3CH_2CH(CH_3)CH_2$ , 1H), 3.45 (OH, 2H), 3.71 (t,  $J = 4.5\text{ Hz}$ ,  $NCH_2CH_2OH$ , 4H), 3.93 (t,  $J = 4.9\text{ Hz}$ ,  $NCH_2CH_2OH$ , 4H), 4.13–4.24 (m,  $CH_3CH_2CH(CH_3)CH_2$ , 2H), 6.79 (d,  $J = 8.9\text{ Hz}$ , 2 aromatic H ortho to  $N(CH_2)_2$ ), 7.86–7.91 (m, 4 aromatic H ortho to  $N=N$ ), 8.13 (d,  $J = 8.4\text{ Hz}$ , 2 aromatic H ortho to  $C(O)OCH_2$ ).

**Scheme 2. Synthetic Route to Azobenzene Monomer of 4-{4-[2-Methyl-3-(2-methylacryloyloxy)propoxy]phenylazo}benzoic Acid 2-Methyl-3-(2-methylacryloyloxy)propyl Ester (Azo3)**



**Synthesis of 4-(4-{Bis-[2-(2-methylacryloyloxy)ethyl]-amino}phenylazo)benzoic Acid 2-Methylbutyl Ester (Azo1):** 4-[4-[Bis(2-hydroxyethyl)amino]phenylazo]benzoic acid 2-methylbutyl ester (100 mg, 0.25 mmol) and methacrylic anhydride (116 mg, 0.75 mmol) were dissolved in acetone (25 mL). A trace of 2,6-di-*tert*-butyl-4-methylphenol was added, and the solution was cooled in an ice bath with stirring. Then a solution of triethylamine (76 mg, 0.75 mmol) and 4-(dimethylamino)pyridine (6 mg, 0.05 mmol) in acetone (10 mL) was added to the first solution drop by drop. The reaction was stirred overnight (14 h) at room temperature. A few drops of acetic acid were added to obtain a pH of 6. The solution was extracted with dichloromethane and washed with water and sodium hydroxide (1 N). The product was purified by column chromatography on silica gel (eluent: AcOEt/hexane = 1.5/8.5). A red oily liquid was obtained: yield 45% (60 mg, 112 mmol); mp  $-26.0$  °C. MS (*m/e*): 535 ( $M^+$ ).  $\lambda_{\max}$  (in THF): 428 nm.  $^1\text{H NMR}$ : 0.95–1.05 (m,  $\text{CH}_3\text{CH}_2\text{CH}(\text{CH}_3)\text{CH}_2$ , 6H), 1.25–1.61 (m,  $\text{CH}_3\text{CH}_2\text{CH}(\text{CH}_3)\text{CH}_2$ , 2H), 1.80–1.90 (m,  $\text{CH}_3\text{CH}_2\text{CH}(\text{CH}_3)\text{CH}_2$ , 1H), 1.93 (s,  $\text{CH}_3\text{C}(\text{CH}_2)\text{C}(\text{O})\text{O}$ , 6H), 3.80 (t,  $J = 6.2$  Hz,  $\text{N}(\text{CH}_2\text{CH}_2\text{O})_2$ , 4H), 4.12–4.26 (m,  $\text{CH}_3\text{CH}_2\text{CH}(\text{CH}_3)\text{CH}_2$ , 2H), 4.39 (t,  $J = 6.1$  Hz,  $\text{N}(\text{CH}_2\text{CH}_2\text{O})_2$ , 4H), 5.59 (s,  $\text{CH}_3\text{C}(\text{CH}_2)\text{C}(\text{O})\text{O}$ , 2H), 6.10 (s,  $\text{CH}_3\text{C}(\text{CH}_2)\text{C}(\text{O})\text{O}$ , 2H), 6.89 (d,  $J = 9.1$  Hz, 2 aromatic H ortho to  $\text{N}(\text{CH}_2)_2$ ), 7.86–7.91 (m, 4 aromatic H ortho to  $\text{N}=\text{N}$ ), 8.15 (d,  $J = 8.5$  Hz, 2 aromatic H ortho to  $\text{C}(\text{O})\text{OCH}_2$ ).

**Synthesis of 4-(4-{Bis(2-acryloyloxyethyl)amino}phenylazo)benzoic Acid 2-Methylbutyl Ester (Azo 2):** The experimental procedure was similar to that for Azo1, except the use of acryloyl chloride instead of methacrylic anhydride; mp:  $-35$  °C. MS (*m/e*): 507 ( $M^+$ ).  $\lambda_{\max}$  (in THF): 428 nm.  $^1\text{H NMR}$ : 0.94–1.05 (m,  $\text{CH}_3\text{CH}_2\text{CH}(\text{CH}_3)\text{CH}_2$ , 6H), 1.25–1.58 (m,  $\text{CH}_3\text{CH}_2\text{CH}(\text{CH}_3)\text{CH}_2$ , 2H), 1.85–1.92 (m,  $\text{CH}_3\text{CH}_2\text{CH}(\text{CH}_3)\text{CH}_2$ , 1H), 3.80 (t,  $J = 6.2$  Hz,  $\text{N}(\text{CH}_2\text{CH}_2\text{O})_2$ , 4H), 4.12–4.36 (m,  $\text{CH}_3\text{CH}_2\text{CH}(\text{CH}_3)\text{CH}_2$ , 2H), 4.40 (t,  $J = 6.1$  Hz,  $\text{N}(\text{CH}_2\text{CH}_2\text{O})_2$ , 4H), 5.82–5.89 (m,  $\text{CH}_2\text{CHC}(\text{O})\text{O}$ , 2H), 6.08–6.17 (m,  $\text{CH}_2\text{CHC}(\text{O})\text{O}$ , 2H), 6.38–6.45 (m,  $\text{CH}_2\text{CHC}(\text{O})\text{O}$ , 2H), 6.88 (d,  $J = 9.2$  Hz, 2 aromatic H ortho to  $\text{N}(\text{CH}_2)_2$ ), 7.86–7.92 (m, 4 aromatic H ortho to  $\text{N}=\text{N}$ ), 8.15 (d,  $J = 8.5$  Hz, 2 aromatic H ortho to  $\text{C}(\text{O})\text{OCH}_2$ ).

**2.2. Preparation of Azo3. Synthesis of 4-(4-Hydroxyphenylazo)benzoic Acid (3):** Aminobenzoic acid (24.5 g, 175 mmol) was dissolved in a mixture of water (344 g) and HCl (60.4 g, 613 mmol), which was cooled in an ice–acetone bath with stirring. A cold solution of  $\text{NaNO}_2$  (13.15 g, 185 mmol) in water (25 g) was added to the first one drop by drop to keep the temperature under 5 °C. Sulfamic acid (1.6 g, 0.017 mmol) was then added to neutralize the oxidant. Afterward, the solution was added to a mixture of AcONa (24.1 g, 175 mmol),  $\text{NH}_4\text{OH}$  (42.3 g, 350 mmol), and phenol (16.65 g, 175 mmol) dissolved in water (335 g). The reaction lasted 1 h at room temperature before addition of acetic acid (30 mL). The solution was filtered, and the product, an orange powder, was rinsed with water and dried. Yield: 95%; mp: decomposed

before melting. MS (*m/e*): 242 ( $M^+$ ).  $\lambda_{\max}$  (in THF): 358 nm.  $^1\text{H NMR}$ : 6.96 (d,  $J = 8.9$  Hz, 2 aromatic H ortho to OH), 7.81–7.85 (m, 4 aromatic H ortho to  $\text{N}=\text{N}$ ), 8.1 (d,  $J = 8.5$  Hz, 2 aromatic H ortho to  $\text{C}(\text{O})\text{OH}$ ).

**Synthesis of 4-[4-(2-Hydroxypropoxy)phenylazo]benzoic Acid 2-Hydroxypropyl Ester (4):** 4-(4-Hydroxyphenylazo)benzoic acid (656 mg, 2.7 mmol) was dissolved in DMF (50 mL), and then (*s*)-(+)-3-bromo-2-methyl-1-propanol (1.45, 9.5 mmol), 1,8-diazabicyclo[5.4.0]undec-7-ene (1.24 g, 8.1 mmol), and potassium iodide (1.35 g, 8.1 mmol) were added to the solution. The solution was stirred and heated to 70 °C for 48 h. The product was collected after extraction of the cold solution with dichloromethane, washing with water and sodium hydroxide (1 N), and recrystallization from toluene solution. Yield: 69%; mp: 130.7 °C. MS (*m/e*): 386 ( $M^+$ ).  $\lambda_{\max}$  (in THF): 362 nm.  $^1\text{H NMR}$ : 1.06–1.09 (m,  $\text{CH}_2\text{CH}(\text{CH}_3)\text{CH}_2$ , 6H), 2.01 (OH, 2H), 2.14–2.24 (m,  $\text{CH}_2\text{CH}(\text{CH}_3)\text{CH}_2$ , 2H), 3.59–3.72 (m,  $\text{CH}(\text{CH}_3)\text{CH}_2\text{OH}$ , 4H), 4.02–4.08 (m,  $\text{C}(\text{O})\text{OCH}_2$ , 2H), 4.33–4.40 (m,  $\text{ArOCH}_2$ , 2H), 7.02 (d,  $J = 7.0$  Hz, 2 aromatic H ortho to  $\text{OCH}_2\text{CH}$ ), 7.89–8.15 (m, 4 aromatic H ortho to  $\text{N}=\text{N}$ ), 8.16 (d,  $J = 7.0$  Hz, 2 aromatic H ortho to  $\text{C}(\text{O})\text{OCH}_2$ ).

**Synthesis of 4-[4-[2-Methyl-3-(2-methylacryloyloxy)propoxy]phenylazo]benzoic Acid 2-Methyl-3-(2-methylacryloyloxy)propyl Ester (AZO 3):** 4-[4-(2-Hydroxypropoxy)phenylazo]benzoic acid 2-hydroxypropyl ester (600 mg, 1.55 mmol) and methacrylic anhydride (838 mg, 5.43 mmol) were dissolved in acetone (55 mL). A trace of 2,6-di-*tert*-butyl-4-methylphenol was added, and the solution was cooled in an ice bath with stirring. A solution of triethylamine (549 mg, 5.43 mmol) and 4-(dimethylamino)pyridine (38 mg, 0.31 mmol) in acetone (15 mL) was added to the first solution drop by drop. The reaction solution was stirred overnight (14 h) at room temperature. A few drops of acetic acid were added to obtain a pH of 6. The monomer was obtained after extraction of the solution with dichloromethane, washing with water and sodium hydroxide (1 N), and purification by column chromatography on silica gel (eluent: AcOEt/hexane = 1/4). Yield: 57% (460 mg, 0.88 mmol); mp: 57 °C. MS (*m/e*): 522 ( $M^+$ ).  $\lambda_{\max}$  (in THF): 360 nm.  $^1\text{H NMR}$ : 1.08–1.18 (m,  $\text{CH}_2\text{CH}(\text{CH}_3)\text{CH}_2$ , 6H), 1.95 (s,  $\text{CH}_3\text{CH}(\text{CH}_2)\text{C}(\text{O})\text{O}$ , 6H), 2.36–2.48 (m,  $\text{CH}_2\text{CH}(\text{CH}_3)\text{CH}_2$ , 2H), 3.96–4.07 (m,  $\text{C}(\text{O})\text{OCH}_2\text{CH}(\text{CH}_3)\text{CH}_2\text{O}$ , 2H), 4.16–4.34 (m,  $\text{C}(\text{O})\text{OCH}_2\text{CH}(\text{CH}_3)\text{CH}_2\text{O}$  and  $\text{OCH}_2\text{CH}(\text{CH}_3)\text{CH}_2\text{O}$ , 6H), 5.58 (s,  $\text{CH}_3\text{C}(\text{CH}_2)\text{C}(\text{O})\text{O}$ , 2H), 6.13 (s,  $\text{CH}_3\text{C}(\text{CH}_2)\text{C}(\text{O})\text{O}$ , 2H), 7.02 (d,  $J = 8.8$  Hz, 2 aromatic H ortho to  $\text{OCH}_2\text{CH}$ ), 7.88–7.99 (m, 4 aromatic H ortho to  $\text{N}=\text{N}$ ), 8.16 (d,  $J = 8.7$  Hz, 2 aromatic H ortho to  $\text{C}(\text{O})\text{OCH}_2$ ).

**3. Preparation of Optically Aligned FLC.** Photoaligned FLC was prepared by polymerizing azobenzene monomers dissolved in the FLC host while exposing the mixture to linearly polarized UV or visible light. The typical procedure is shown in the following example. In a small flask, Azo1 (1.8 mg, 0.0034 mmol), FLC (60 mg), and AIBN (1.2 mg) were dissolved in THF (0.3 mL) at room temperature to obtain a

homogeneous solution. The solvent was allowed to evaporate at room temperature first under the atmosphere pressure for 10–14 h and then in a vacuum oven for 3 h. A drop of the freshly dried mixture was then placed between two quartz plates, warmed to 40 °C, and compressed manually to produce a film of about 60 mm<sup>2</sup> large and with a thickness around 5 μm. Afterward, the film was moved into a microscope hot stage and, without delay, exposed to linearly polarized light (normal incidence) while being heated to 110 °C in the isotropic phase for 15 min to complete the thermally induced free radical polymerization of the azobenzene monomer. With a heating rate of about 20 °C/min, polymerization started during the heating but was essentially preceded in the isotropic phase. Finally, under irradiation the mixture was cooled, at a rate of about 5 °C/min, to room temperature. After the preparation procedure was completed, the irradiation light was turned off. All samples prepared using this procedure were first examined on a polarizing optical microscope to observe the photoalignment of FLC and then used in different experiments as shown in the paper.

The concentration of azobenzene monomer in the FLC was between 1 and 10 wt %. Linearly polarized irradiation light was obtained by using an UV–vis curing system (Novacure) combined with an UV or visible interference filter (10 nm bandwidth, Oriel) and an UV linear dichroic polarizer (Oriel). Both polarized UV irradiation at 360 nm (~10 mW/cm<sup>2</sup>) and polarized visible exposure at 440 nm (~4 mW/cm<sup>2</sup>) were produced. For all experiments of photoisomerization and photoalignment in this study, polarized UV light was used for Azo3, whereas polarized visible light was used for Azo1 and Azo2.

**4. Characterizations. Monomers:** All azobenzene monomers as well as the compounds used for their synthesis were characterized by a number of techniques. Their <sup>1</sup>H NMR spectra in CDCl<sub>3</sub> were recorded on a Bruker-AC300 (300 MHz) or a Bruker DMX-600 (600 MHz) spectrometer. Mass spectra were recorded on a Micromass ZAB-1F high-resolution mass spectrometer. A differential scanning calorimeter (Perkin-Elmer DSC-7) was used to investigate their thermal behavior, using indium as the calibration standard and a heating or cooling rate of 10 °C/min. All compounds were found to display only a crystalline phase before melting. Their reported melting temperature was determined as the maximum of the endothermic peak during the second heating scan. UV–vis spectra in THF solution were recorded on a Hewlett-Packard 8452A diode array spectrophotometer.

**Mixtures of Monomer/FLC and Polymerized Samples:** DSC was also used to monitor the polymerization of the azobenzene monomers dissolved in the FLC. In each case, a freshly dried mixture (about 15 mg) was inserted into a DSC pan, and the first heating scan was recorded from 20 to 160 °C to complete the polymerization. Then the sample was cooled to room temperature, and a second heating scan was conducted to observe the changes. A polarizing optical microscope (Leitz DMR-P, magnification 100×) equipped with an Instec hot stage was used to examine the photoalignment of FLC after the irradiation light was turned off at room temperature (see the conditions described above for the preparation of optically aligned samples). Optical micrographs were taken using a Leica DC-300 digital camera. The photoisomerization of azobenzene monomers (before polymerization) and polymers (after polymerization) in the FLC was also investigated using the UV–vis spectrophotometer. UV–vis spectra of thin films (about 5 μm thick) cast between two quartz plates were recorded immediately after the UV or visible irradiation, and for polarized UV–vis measurements, a polarizer (Oriel) was placed in front of the optically aligned sample. Finally, a scanning electron microscope (JEOL JSC-840A) was used to observe the azobenzene polymer networks. For these experiments, the films between quartz plates were dipped in hexane to slowly remove the FLC; the two plates were then carefully separated, and the polymer network remained on both substrates was dried before use.

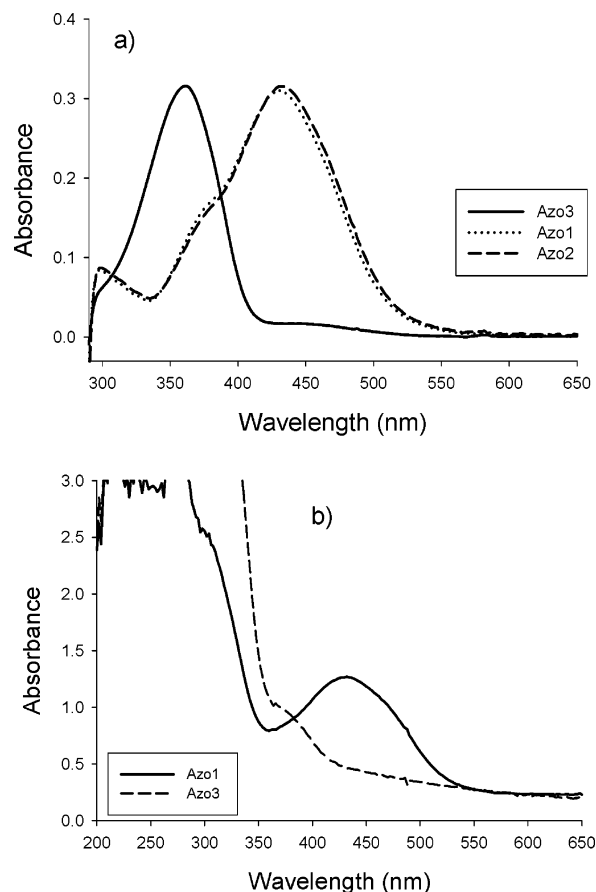


**Figure 2.** UV–vis spectra of azobenzene monomers in (a) tetrahydrofuran solution and (b) the ferroelectric liquid crystal.

## Results and Discussion

**1. Chiral Azobenzene Monomers.** The UV–vis spectra of all azobenzene monomers dissolved in THF are shown in Figure 2a. Because of the electron-donor and electron-acceptor groups, Azo1 and Azo2 have the maximum absorption of *trans*-azobenzene ( $\pi$ – $\pi^*$  transition) appearing in the visible region (428 nm), whereas Azo3 displays the maximum absorption ( $\pi$ – $\pi^*$  transition) at lower wavelengths in the UV range (360 nm) and weak absorption in the visible range (450 nm,  $n$ – $\pi^*$  transition). Given in Figure 2b are the UV–vis spectra of 5% Azo1 and 3% Azo3 dissolved in the FLC host. For Azo1 and Azo2, the absorption band of azobenzene shows little shift in the FLC (432 nm) and is well separated from the strong absorption of the latter at lower wavelengths, while the absorption of Azo3 in the FLC is noticed as a shoulder due to overlapping of FLC. For all monomers, the occurrence of photoisomerization at the used irradiation wavelengths was confirmed.

The chiral nature of all monomers was confirmed by mixing them with a nematic LC. They all act as a chiral dopant and induce a chiral nematic (N\*) phase. Figure 3 shows polarizing optical micrographs for a nematic LC, BL006 (Merck), containing 5% azobenzene monomer, taken at 100 °C. The fingerprint texture characteristic of the induced N\* phase is observed in all mixtures. Moreover, a stronger helical twisting in the mixture with Azo3 is clearly the result of a higher concentration of chiral centers, twice as many as Azo1 and Azo2. The helical pitch estimated from Figure 3 is about 6.6 μm with Azo3 and 12 μm for both Azo1 and Azo2. Note that if an initiator (AIBN) is added in the

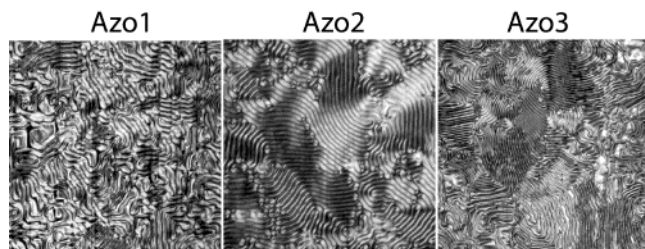


**Figure 3.** Polarizing optical micrographs, taken at 100 °C, of 5% azobenzene monomers dissolved in a nematic liquid crystal. The fingerprint texture arises from the induced chiral nematic phase. Picture area: 470  $\mu\text{m}$   $\times$  470  $\mu\text{m}$ .

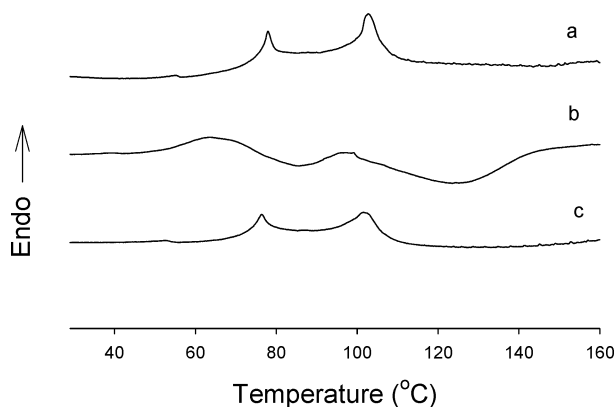


**Figure 4.** DSC heating curves (10 °C/min): (a) second heating scan for the pure ferroelectric liquid crystal (FLC); (b) first heating scan for the mixture of FLC with 5% 4-(4-{bis-[2-(2-methylacryloyloxy)ethyl]amino}phenylazo)benzoic acid 2-methylbutyl ester (Azo1); and (c) second heating scan for the mixture of FLC/Azo1 (5%).

mixture for polymerization, the conversion of the chiral monomer into a chiral polymer network reduces the chirality transfer to the nematic BL006, and most helices are unwinded.

**2. Polymerization and Polymer Networks in FLC.** Before investigating the optical alignment of FLC, we performed a series of experiments without irradiation to make sure that polymerization of all chiral monomers did take place in the FLC and give rise to polymer networks. Figure 4 compares the DSC heating curves of the pure FLC and its mixture with 5% azobenzene monomer, Azo1. The occurrence of polymerization during the first heating scan of the mixture is clearly revealed by the exotherm starting at about 65 °C, which is superimposed with the mesophase transition endothermic peaks of the FLC. It is noticeable that the  $S_A-N^*$  and  $N^*-I$  transition temperatures in the mixture with the monomer are lowered by several degrees as compared with that of the pure FLC, which is caused by a disrupting effect of the monomer dissolved in the FLC. After polymerization, on the second heating scan, only the transition peaks are observed, and the transition temperatures rebound but still remain lower than those of pure FLC due to the interaction between the FLC and polymer network. These results indicate that the azobenzene monomer is dissolved in the FLC and can be polymerized at temperatures in either the  $N^*$  or the isotropic phase. Similar results were obtained for other monomers.

The formation of an azobenzene polymer network can also be observed on an optical microscope. After polymerization in the isotropic phase (110 °C), a uniform liquid film is seen on bright field, which is orange-

colored due to the azobenzene chromophore, and no phase separation can be detected. This suggests a fine dispersion of the formed polymer network in the FLC. However, when the mixture is cooled into the LC phases, where the liquid crystal domains develop, the polymer network apparently is segregated from the FLC and move into the many defect or disclination regions associated with the polydomain structure (no bulk alignment). On reheating the mixture into the isotropic phase, the thickened polymer network becomes visible on the bright-field optical microscope, as is shown in Figure 5. It is apparent that the azobenzene polymer networks have different morphologies, depending on the chemical structure of the azobenzene monomer. Azo1 gives the most prominent 3D-like network, with connection of long and flexible filaments. The polymer of Azo2 seems to be concentrated in certain areas, while for Azo3 the network appears as an assembly of short and irregularly shaped aggregates. SEM observations confirmed the formation of very different polymer networks. Figure 6 shows SEM images of networks formed from polymerization of 3% monomer in the mixture, the FLC host being extracted in hexane. Even though these pictures may not reflect the exact state of the network in the FLC because alternations such as collapse may happen during the FLC removal, the differences are evident. For Azo1, the network is formed by long strings of interconnected spherical particles (about 250 nm in diameter); it is likely that such strings of particles may be flexible and easy to arrange into a uniform and open network structure. In the case of Azo2, larger and compact-looking aggregates coexist with noninterconnected particles of irregular shapes, and the network of Azo3 is formed by twisted aggregates of rice-grain particles. These features are consistent with the optical microscopic observations (Figure 5). As is shown below, the polymer network morphology has profound effects on the optical alignment of FLC. It was noted that the polymerization kinetics of the three azobenzene monomers in the FLC, as revealed by the nonisothermal DSC measurements (exemplified in Figure 4), showed no noticeable differences. Moreover, using Azo1, it was found by SEM that similar morphology resulted from polymerizations carried out at different temperatures in the isotropic phase. These results suggest that the different polymer networks formed from the three monomers should mainly be caused by different polymer interactions and compatibility with the FLC, which affect the phase separation behavior. The more twisted network structure of Azo3 may be related to the greater chirality of this monomer than Azo1 and Azo2.

**3. Photoalignment of FLC.** As mentioned earlier, the photoisomerization and photoalignment of the azobenzene chromophore were thought of as what may impart a bulk alignment of FLC contained by an azobenzene polymer network. The photoisomerization of azobenzene monomers as well as azobenzene moieties on the polymer network in the FLC host was confirmed by UV-vis spectroscopy. An example is given in Figure 7, displaying changes in the UV-vis spectrum of 5% Azo1 polymerized in the FLC, upon irradiation at 440 nm. The *trans*-*cis* isomerization of azobenzene moieties on the network (likely on the surface) is indicated by the diminution of the absorption of *trans*-azobenzene around 432 nm, which is almost superimposed with the  $n-\pi^*$  transition of *cis*-azobenzene at about 450 nm.

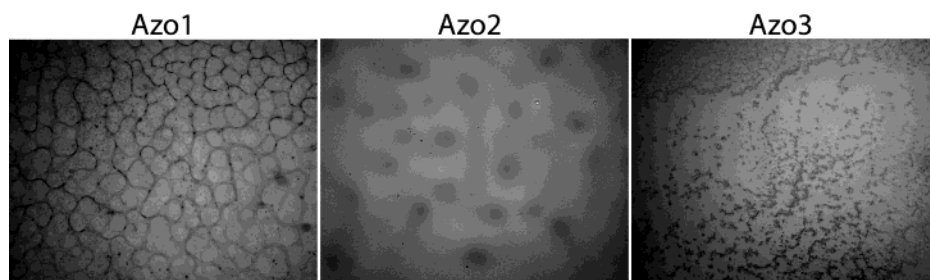


**Figure 5.** Azobenzene polymer networks formed by 3% monomer dissolved in the ferroelectric liquid crystal, viewed on bright field optical microscope at 110 °C. Picture area: 780  $\mu\text{m}$   $\times$  625  $\mu\text{m}$ .

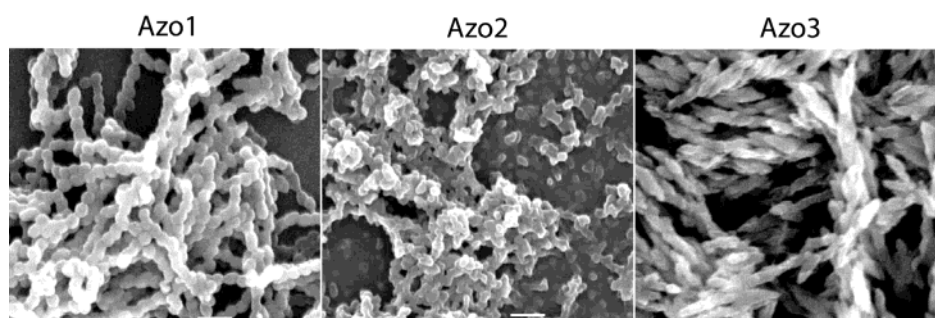


**Figure 6.** Scanning electron microscope images of azobenzene polymer networks formed from 3% monomer dissolved in the ferroelectric liquid crystal (FLC). The FLC host was removed in hexane. The scale bar is 1  $\mu\text{m}$ .

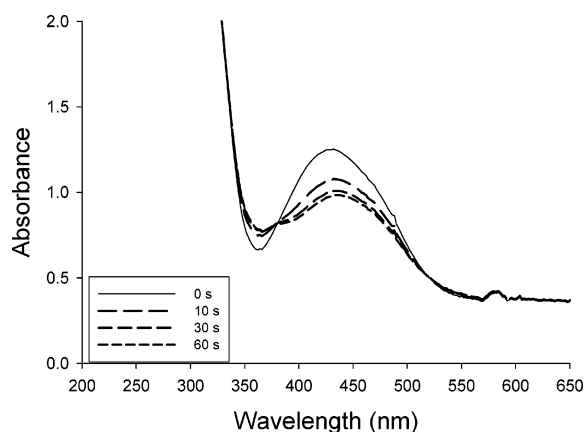


**Figure 7.** UV-vis spectra for a sample of ferroelectric liquid crystal with 5% azobenzene polymer network formed from 4-(4-{bis-[2-(2-methylacryloyloxy)ethyl]amino}phenylazo)benzoic acid 2-methylbutyl ester (Azo1) before and after irradiation. Irradiation times are indicated.

Mention also that in another series of experiments photoinduced birefringence was observed for mixtures of chiral azobenzene monomers and polymers (except Azo3) in a FLC similar to the one used in this study (excitation using an Ar<sup>+</sup> laser at 488 nm).<sup>24</sup> All these confirm the occurrence of the photoisomerization of azobenzene monomers as well as azobenzene moieties on the polymer networks in the FLC. As shown later, a preferential orientation of azobenzene groups in the direction perpendicular to the polarization of irradiation light may be induced as a result of the conventional photoorientation process.

Of the three chiral azobenzene monomers, Azo1 and Azo2 were found to be able to induce optically aligned FLC without rubbed surfaces. Azo3 cannot. Using the mixture with 1% Azo2, Figure 8 illustrates the conditions and the typical results. Whatever the azobenzene monomer used, a good dissolution or fine dispersion in the FLC host is indispensable for the success of photoalignment. Quite surprisingly, the chiral monomers

actually have a strong tendency to be phase separated from the FLC at room temperature. If the phase separation precedes the polymerization under linearly polarized irradiation, no bulk alignment of FLC can be achieved. It is therefore crucial to carry out the experiment on freshly prepared homogeneous mixtures. Quick evaporation of the solvent was found to be effective to produce a kinetically controlled homogeneous mixture. Figure 8a shows the apparent texture of such a mixture compressed between two quartz plates, with no developed smectic texture. From this state, if the mixture is heated to the isotropic phase and cooled back to room temperature without irradiation, the monomer is simply polymerized, but there is no bulk alignment of FLC in the S<sub>c</sub>\* phase (Figure 8b). If linearly polarized irradiation is applied to the mixture during the whole process of heating and cooling, a bulk alignment of smectic domains can be obtained along the direction perpendicular to the polarization of irradiation light (Figure 8c). Clearly this optical alignment of FLC must be attributed to the action of azobenzene moieties.

Better photoinduced bulk alignment of FLC was observed using Azo1 than with Azo2. Figure 9 shows the representative results at various concentrations of Azo1. Good alignment was obtained with up to 5% Azo1, but a higher concentration leads to more defects, where the azobenzene polymer network is located. No bulk alignment was observed with 10% Azo1, the polymer network of which seems to be too dense to allow the alignment to develop. Two significant differences emerged between chiral and achiral azobenzene polymers investigated for the photoalignment of FLC. First, in the case of the achiral polymer network,<sup>17,18</sup> there is an enhanced segregation of the polymer network from aligned FLC in the S<sub>c</sub>\* phase, which results in the appearance of thick polymer threads (~ several micrometers in width) running parallel to the aligned smectic domains. No such increased phase separation was observed for aligned FLC with the chiral azobenzene polymer networks.

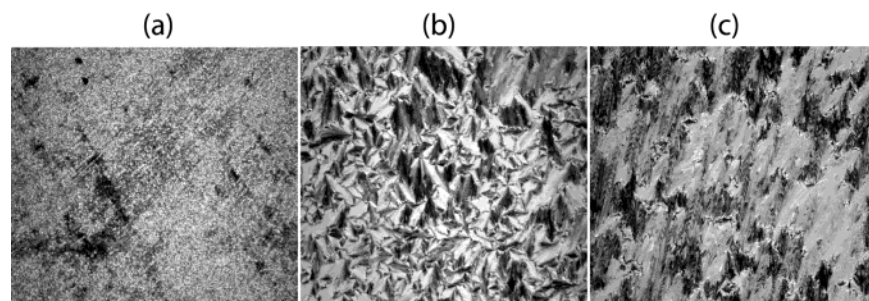


**Figure 8.** Polarizing optical micrographs for a film of the mixture of ferroelectric liquid crystal and 5% 4-[4-[bis(2-acryloyloxyethyl)-amino]phenylazo]benzoic acid 2-methylbutyl ester (Azo2) at room temperature: (a) before polymerization and irradiation; (b) after polymerization without irradiation; and (c) after polymerization under irradiation. Picture area:  $780 \mu\text{m} \times 700 \mu\text{m}$ .

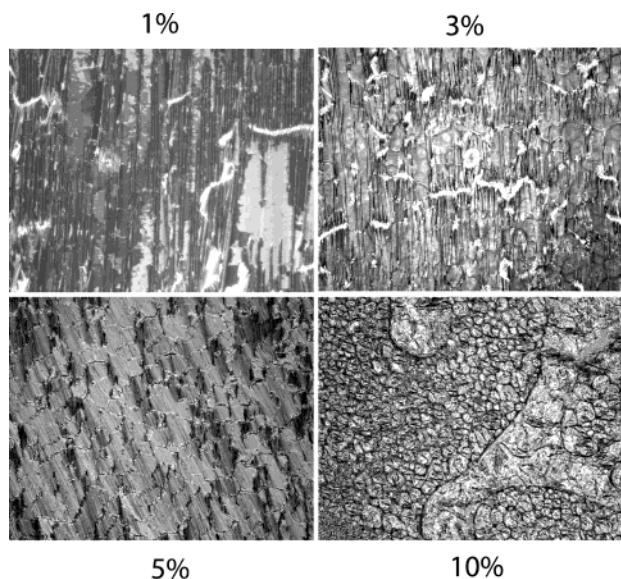


**Figure 9.** Photoinduced bulk alignment of ferroelectric liquid crystal in the chiral smectic C phase ( $S_C^*$ ) using various concentrations of azobenzene polymer network formed from 4-(4-[bis-[2-(2-methylacryloyloxy)ethyl]amino]phenylazo)-benzoic acid 2-methylbutyl ester (Azo1). The alignment of smectic domains is perpendicular to the polarization of irradiation light. Picture area:  $860 \mu\text{m} \times 700 \mu\text{m}$ .

Second, the chiral azobenzene polymer network exerts a commanding effect on the alignment of FLC, since photoinduced reorientation can be achieved by changing the polarization direction of irradiation light, which was not observed for achiral azobenzene polymer networks. Some results are presented in Figure 10 to explain the way it works. All samples were first photoaligned in one direction. Then, after covering a part of the sample (the upper part in the photos) by an aluminum sheet, the film was exposed to a second irradiation with the polarization rotated by  $90^\circ$ , and during the process the film was heated either to the  $N^*$  phase ( $90^\circ\text{C}$ ) or the isotropic phase ( $110^\circ\text{C}$ ) before being cooled to room temperature. Polarizing photomicrographs a and b show the  $90^\circ$  reorientation of smectic domains in the uncovered lower part for a film containing 1% Azo1 heated to the  $N^*$  and isotropic phase, respectively. In the latter case, the initial horizontal alignment in the covered area was lost after the isotropization process. The reorientation occurred in the  $N^*$  phase for a sample with 3% Azo1 is shown in photo c. Because of the higher concentration of azobenzene polymer network, the reorientation boundary between the two areas appears less sharper. Photo d is for the same sample as in photo c but was taken after removal of crossed polarizers. On bright field, the orange-colored azobenzene polymer network becomes

visible. The network appears randomly aligned and displays no noticeable difference in the two areas with orthogonal alignment of smectic domains. Moreover, SEM observations made on aligned samples found no evidence of anisotropic polymer network. A typical result is shown in Figure 11, obtained after extraction of FLC from an aligned FLC with 3% Azo1. At higher magnifications, the formation of network by interconnected spherical particles, like in Figure 6, could be seen.

Polarized UV-vis spectroscopic measurements confirmed that the reorientation of smectic domains described above is related to the photoinduced reorientation of azobenzene moieties on the polymer network. Figure 12 shows the angular dependence of the absorbance of azobenzene moieties at 432 nm for a sample with 3% Azo1, before and after the reorientation. The angle is that between the polarizations of the beam of spectrophotometer and the irradiation light used for the first irradiation. Within experimental errors, the highest absorbance found at  $90^\circ$  after the first irradiation indicates the orientation of azobenzene moieties in the expected direction, i.e., perpendicular to the polarization of irradiation light, which is also the alignment direction of smectic domains. After the second irradiation with the polarization changed by  $90^\circ$ , the results in Figure 12 show a  $90^\circ$  reorientation of azobenzene moieties that correlates with the observed  $90^\circ$  rotation of the smectic domains (Figure 10). Some other features about this photoinduced reorientation of FLC need to be emphasized. On one hand, the reorientation process takes place only when the sample is heated to either the  $N^*$  phase or the isotropic phase, while it does not happen in both the smectic A ( $S_A$ ) and the  $S_C^*$  phase. This is understandable because the reorientation of smectic domains, which have higher molecular order and rotational viscosity than the nematic phase, through photoalignment of azobenzene is more energetically demanding than reorienting nematic domains. The difficulty of reorienting initially ordered LC domains is known even with the azobenzene chromophore as part of the LC structure.<sup>25</sup> While in the present case, the azobenzene polymer is phase-separated from the FLC, and the effect of photoalignment of azobenzene on the surrounding FLC molecules would be provided mainly by azobenzene moieties on the surface of the network. On the other hand, if the aligned sample is heated to the isotropic phase and cooled without irradiation, the initial orientation cannot be recovered. In other words, the orientational memory effect, known for anisotropic polymer networks,<sup>11</sup> is absent for optically aligned FLC with the chiral azobenzene network.

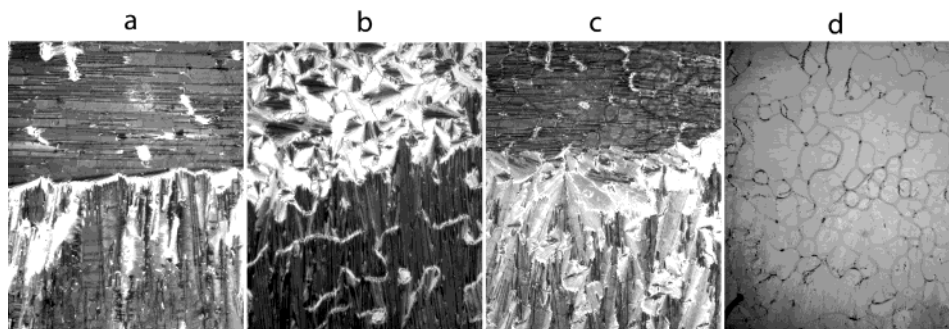


**Figure 10.** Optical micrographs at room temperature showing photoinduced reorientation of ferroelectric liquid crystal by changing polarization of irradiation light: (a) 1% azobenzene polymer network formed from 4-(4-{bis-[2-(2-methylacryloyloxy)ethyl]amino}-phenylazo)benzoic acid 2-methylbutyl ester (Azo1) with reorientation occurred in the  $N^*$  phase; (b) 1% Azo1 with reorientation occurred in the isotropic phase; (c) 3% Azo1 with reorientation occurred in the  $N^*$  phase; and (d) bright field picture for the same film as in (c). See text for details. Picture area:  $625 \mu\text{m} \times 770 \mu\text{m}$ .

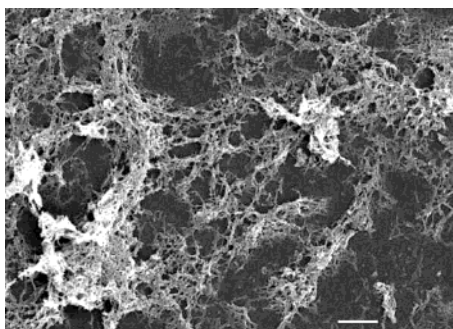


**Figure 11.** Scanning electron microscope image of the azobenzene polymer network formed from 3% 4-(4-{bis-[2-(2-methylacryloyloxy)ethyl]amino}phenylazo)benzoic acid 2-methylbutyl ester (Azo1) in an aligned ferroelectric liquid crystal. The scale bar is  $10 \mu\text{m}$ .

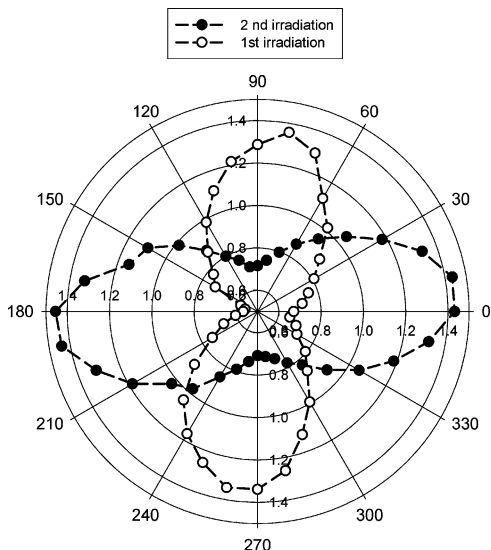


**Figure 12.** Angular dependence of absorbance of azobenzene moieties on the network at  $432 \text{ nm}$  for an aligned ferroelectric liquid crystal containing 3% azobenzene polymer network formed from 4-(4-{bis-[2-(2-methylacryloyloxy)ethyl]amino}-phenylazo)benzoic acid 2-methylbutyl ester (Azo1) after two irradiations with the polarization changed by  $90^\circ$ .

All the results together suggest a different mechanism for the photoinduced alignment of FLC from the chiral Azo1 polymer network, which is schematically illustrated in Figure 13. The network is isotropic and formed by connection of spherical polymer particles, whose colloidal dimension ( $\sim 250 \text{ nm}$  diameter) ensures a high surface-to-volume ratio and thereby a large number of

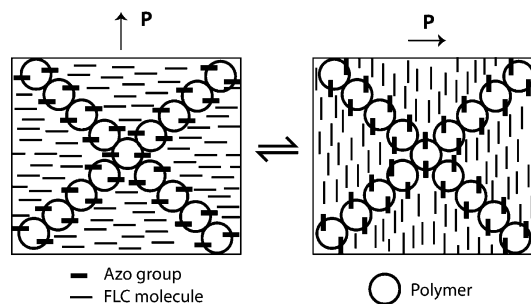


**Figure 13.** Schematic illustration of the photoinduced reorientation of ferroelectric liquid crystal with a network of colloidal particles of azobenzene polymer.

surface azobenzene moieties that can undergo the photoisomerization. The photoinduced alignment of the surface azobenzene moieties under linearly polarized irradiation may bring the FLC molecules in the  $N^*$  phase to align in the same direction, and this alignment remains in the lower-temperature  $S_A$  and  $S_C^*$  phases. Changing the polarization of irradiation light changes the orientation of the surface azobenzene moieties and, as a result, reorients the FLC molecules. When such an aligned sample is heated into the isotropic phase without irradiation, the orientation of azobenzene groups would be relaxed, and subsequent cooling into the LC phases cannot recover the initial bulk alignment of FLC. It is easy to picture that a uniform network of strings of colloidal particles would maximize the interaction with the surrounding FLC molecules leading to effective alignment of FLC. This appears to be the case for the chiral Azo1 polymer network (Figures 6 and 11). The observed differences between chiral and achiral azobenzene polymers are likely to find the origin in the interactions between the network and the FLC. As mentioned in Introduction, it was anticipated that chiral azobenzene polymers might have an enhanced compatibility with the chiral FLC host, which affects the morphology of polymer network after phase separation and, consequently, the photoalignment behavior of the FLC.

Contrarily to Azo1, the absence of photoalignment of FLC using Azo3 may be explained by a combination of several of factors. First, the overlap of the absorption of Azo3 with that of the FLC host may reduce its excitation and hinder its photoalignment. Second, in contrast with Azo1 and Azo2, the lack of electron-donor and electron-acceptor substituents on the azobenzene unit of Azo3 results in the poor overlap of  $\pi-\pi^*$  and  $n-\pi^*$  absorptions (Figure 2) and longer lifetime of the *cis*

isomer, the consequence of which is a less efficient photoinduced orientation of azobenzene moieties.<sup>25</sup> Third, probably more damaging for the Azo3 polymer network is the fact that azobenzene moieties are part of chain backbone by fixation of both ends. The lack of freedom for azobenzene moieties on the surface may also prevent their photoalignment from happening. In another study using azobenzene divinyl ethers and diepoxides,<sup>26</sup> photoalignment of FLC was observed for monomers with similar structures. However, as compared with these monomers, the shorter spacers of Azo3, which bear two chiral centers, may restrict the mobility of azobenzene moiety. Finally, note that the surface property of the substrate has a profound effect on the photoalignment of FLC. Best results were achieved so far with untreated quartz plates, whereas only partial alignment was obtained with glass plates coated with indium–tin oxide (ITO). Work is underway to modify the surface tension of ITO in order to obtain uniform photoalignment of FLC required for electrooptical measurements.

### Conclusions

Three chiral dimethacrylate and diacrylate monomers containing an azobenzene group in their structure were synthesized and investigated for photoinduced alignment of FLC in the absence of surface orientation layers. When dissolved in a FLC host and polymerized under linearly polarized irradiation, two of the monomers are able to induce a bulk alignment of FLC in the  $S_C^*$  phase, with a concentration as low as 1%. Polymerization of the monomer Azo1, which is most effective in inducing photoalignment, results in a polymer network formed by strings of colloidal particles with diameters in the range of 250 nm. Experimental evidence suggests that the photoinduced bulk alignment of FLC related to the chiral azobenzene polymer networks may be achieved through a different mechanism as compared with achiral azobenzene polymers.<sup>14–18</sup> Instead of the anisotropic polymer network observed in the latter case, which serves as a framework for the induction and stabilization of FLC, the network from chiral Azo1 may be isotropic, and it is the photoinduced orientation of the large number of azobenzene moieties on the surface of the network, i.e., at the interface with the FLC, that is responsible for the alignment of FLC. This mechanism accounts for the observed reorientation of FLC by changing the polarization of irradiation light as well as the absence of the orientational memory effect characteristic of an anisotropic network. In such azobenzene polymer-stabilized FLC, since the polymer network is

dispersed in the host, the action of the surface azobenzene moieties actually provides a volume effect on the surrounding FLC molecules, which is different from the so-called commanding surfaces by optically aligning azobenzene groups of thin layers coated on the substrate.<sup>6</sup>

**Acknowledgment.** We thank the Natural Sciences and Engineering Research Council of Canada and le Fonds québécois de la recherche sur la nature et les technologies (Québec) for financial support.

### References and Notes

- (1) Yang, D.-K.; Chien, L. C.; Fung, Y. K. In *Liquid Crystals in Complex Geometries Formed by Polymer and Networks*; Crawford, G. P., Zumer, S., Eds.; Taylor & Francis: London, 1996; pp 103–143.
- (2) Hikmet, R. A. M. In ref 1, pp 53–83.
- (3) Hikmet, R. A. M. *Adv. Mater.* **1995**, *7*, 300.
- (4) Guymon, C. A.; Dougan, L. A.; Martens, P. J.; Clark, N. A.; Walba, D. M.; Bowman, C. N. *Chem. Mater.* **1998**, *10*, 2378.
- (5) Natansohn, A.; Rochon, P.; Gosselin, J. J.; Xie, S. *Macromolecules* **1992**, *25*, 2268.
- (6) Kim, D. Y.; Li, L.; Jiang, X. L.; Shivshankar, V.; Kumar, J.; Tripathy, S. K. *Macromolecules* **1995**, *28*, 8835.
- (7) Ichimura, K. *Chem. Rev.* **2000**, *100*, 1847.
- (8) Eich, M.; Wendorff, J. H. *Makromol. Chem. Rapid Commun.* **1987**, *8*, 59.
- (9) Wu, Y.; Zhang, Q.; Kanazawa, A.; Shiono, T.; Ikeda, T.; Nagase, Y. *Macromolecules* **1999**, *32*, 3951.
- (10) Fischer, T.; Lasker, L.; Stumpe, J.; Kostromin, S. *Photochem. Photobiol. A: Chem.* **1994**, *80*, 453.
- (11) Bai, S.; Zhao, Y. *Macromolecules* **2001**, *34*, 9032.
- (12) Zhao, Y.; Bai, S.; Dumont, D.; Galstian, T. *Adv. Mater.* **2002**, *14*, 512.
- (13) Bai, S.; Zhao, Y. *Macromolecules* **2002**, *35*, 9657.
- (14) Corvazier, L.; Zhao, Y. *Macromolecules* **1999**, *32*, 3195.
- (15) Zhao, Y.; Chenard, Y.; Paiement, N. *Macromolecules* **2000**, *33*, 1049.
- (16) Zhao, Y.; Chenard, Y. *Macromolecules* **2000**, *33*, 5891.
- (17) Zhao, Y.; Paiement, N. *Adv. Mater.* **2001**, *13*, 1891.
- (18) Zhao, Y.; Paiement, N.; Sévigny, S.; Leclair, S.; Motallebi, S.; Giguère, M.; Bouchard, L. *SPIE Proc.* **2003**, *5003*, 150.
- (19) Clark, N. A.; Larerwall, S. T. *Appl. Phys. Lett.* **1980**, *36*, 899.
- (20) Molsen, H.; Kitzrow, H.-S. *J. Appl. Phys.* **1994**, *15*, 710.
- (21) Mao, G.; Wang, J.; Ober, C. K.; Brehmer, M.; O'Rourke, M. J.; Thomas, E. L. *Chem. Mater.* **1998**, *10*, 1538.
- (22) Semmler, K.; Finkelmann, H. *Macromol. Chem. Phys.* **1995**, *196*, 3197.
- (23) Brehmer, M.; Zentel, R. *Macromol. Chem. Phys.* **1994**, *195*, 1891.
- (24) Unpublished results obtained using Felix015, another FLC from Clariant.
- (25) Natansohn, A.; Rochon, P. *Chem. Rev.* **2002**, *102*, 4139.
- (26) Sévigny, S.; Bouchard, L.; Motallebi, S.; Zhao, Y. *Macromolecules* **2003**, *36*, 9033.MA034886D

MA034886D